



**HAL**  
open science

## A Dy<sub>4</sub> Cubane A New Member in the Single-Molecule Toroics Family

Guglielmo Fernandez Garcia, Djamilla Guettas, Vincent Montigaud, Paolo Larini, Roberta Sessoli, Federico Totti, Olivier Cador, Guillaume Pilet, Boris Le Guennic

► **To cite this version:**

Guglielmo Fernandez Garcia, Djamilla Guettas, Vincent Montigaud, Paolo Larini, Roberta Sessoli, et al.. A Dy<sub>4</sub> Cubane A New Member in the Single-Molecule Toroics Family. *Angewandte Chemie International Edition*, 2018, 57 (52), pp.17089-17093. 10.1002/anie.201810156 . hal-01937239

**HAL Id: hal-01937239**

**<https://univ-rennes.hal.science/hal-01937239>**

Submitted on 3 Dec 2018

**HAL** is a multi-disciplinary open access archive for the deposit and dissemination of scientific research documents, whether they are published or not. The documents may come from teaching and research institutions in France or abroad, or from public or private research centers.

L'archive ouverte pluridisciplinaire **HAL**, est destinée au dépôt et à la diffusion de documents scientifiques de niveau recherche, publiés ou non, émanant des établissements d'enseignement et de recherche français ou étrangers, des laboratoires publics ou privés.

# A Dy<sub>4</sub> Cubane: A New Member in the Single-Molecule Toroids Family

Guglielmo Fernandez Garcia,<sup>[a,b]</sup> Djamilla Guettas,<sup>[c]</sup> Vincent Montigaud,<sup>[a]</sup> Paolo Larini,<sup>[d]</sup> Roberta Sessoli,<sup>[b]</sup> Federico Totti,<sup>[b]</sup> Olivier Cador,<sup>\*[a]</sup> Guillaume Pilet,<sup>\*[c]</sup> and Boris Le Guennic<sup>\*[a]</sup>

**Abstract:** Molecular materials that possess a toroidal moment associated to a non-magnetic ground state are known as Single-Molecule Toroids (SMTs) and are usually planar molecules. Herein, we report a Dy<sub>4</sub> cubane, namely [Dy<sub>4</sub>(Bppd)<sub>4</sub>(μ<sub>3</sub>-OH)<sub>4</sub>(PaH)<sub>4</sub>(H<sub>2</sub>O)<sub>4</sub>]·0.333H<sub>2</sub>O (where BppdH=1,3-Bis(pyridin-4-yl)propane-1,3-dione and PaH=2-Picolinic acid) for which magnetometry measurements and state-of-art ab initio calculations highlight SMT behavior in a tridimensional structure (3D-SMT). The in-depth theoretical analysis on the resulting low-lying energy states, along with their variation in function of the magnetic exchange pathways, allows to shed further light on the description of Single-Molecule Toroids and identify the coupling scheme that better reproduce the observed data.

Single Molecule Magnet (SMM) behavior was discovered more than twenty years ago in polynuclear 3d complexes<sup>[1]</sup> and ten years later, in mononuclear 4f complexes,<sup>[2]</sup> the latter being nowadays the most popular.<sup>[3]</sup> These objects fascinate chemists and physicists because they might be components of spintronic devices.<sup>[4,5]</sup> They are conceptually based on axial magnetic anisotropy to create a potential barrier separating the two orientations of the magnetic moment. Magnetic orbitals of lanthanide are largely subject to spin-orbit coupling but slightly perturbed by the coordination because of the small radial extension of 4f orbitals. Therefore, the amplitude of the magnetic anisotropy is much stronger for lanthanide ions and this turns to be an advantage to produce mononuclear SMMs.<sup>[6]</sup> However, the fast relaxation observed in these systems at zero magnetic field is a long-standing problem.<sup>[7]</sup> To overcome it, the suppression of hyperfine couplings through isotopic substitution and the dilution in diamagnetic matrices are efficient alternatives.<sup>[8,9]</sup> Another strategy resides in having inside the

molecule more than one paramagnetic center coupled through exchange interactions. The magnetic interactions between lanthanide magnetic moments in homometallic polynuclear complexes are, in general, very small (of the order of few Kelvin)<sup>[10,11]</sup> and not always able to quench the tunneling relaxation process between the two low-lying exchange multiplets, even if radical ligands strongly modify this picture.<sup>[12]</sup> Indeed parallel and axial principal magnetic axes of the individual centers are needed.<sup>[13]</sup> On the other hand, polynuclear lanthanide systems can show very peculiar magnetic moments configurations at low temperature which are due to a subtle balance between anisotropy directions and exchange interactions.

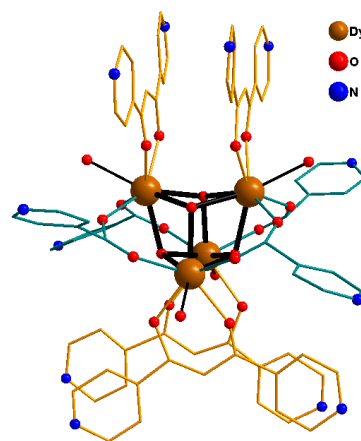


**Figure 1.** Representation of the crystal structure of Dy<sub>4</sub>. BppdH are in yellow rods, PaH in green rods, while Dy, O and N are in gold, red and blue balls, respectively. Hydrogen atoms have been omitted for clarity.

[a] Dr. G. Fernandez Garcia, V. Montigaud, Prof. Dr. O. Cador, Dr. B. Le Guennic

Institut des Sciences Chimiques de Rennes  
UMR 6226 CNRS-Université de Rennes 1  
263 Avenue du Général Leclerc, 35042 Rennes Cédex (France)  
E-mail: olivier.cador@univ-rennes1.fr  
boris.leguennic@univ-rennes1.fr

[b] Prof. Dr. R. Sessoli, Dr. F. Totti  
Dipartimento di Chimica 'Ugo Schiff  
Università degli Studi di Firenze  
Via della Lastruccia 3-13, Sesto Fiorentino 50019 (Italy)

[c] Dr D. Guettas, Dr. G. Pilet  
Laboratoire des Multimatiériaux et Interfaces (LMI)  
UMR 5615 CNRS-Université Claude Bernard Lyon 1  
Bâtiment Chevreul, Avenue du 11 novembre 1918, 69622  
Villeurbanne cedex (France)  
E-mail: guillaume.pilet@univ-lyon1.fr

[d] Dr. P. Larini  
Institut de Chimie de Lyon, C2P2  
UMR 5265 CNRS-CPE Lyon-UCBL  
43 Bd du 11 Novembre 1918, 69616 Villeurbanne (France)

Supporting information for this article is given via a link at the end of the document

Probably, Single-Molecule Toroids (SMTs) are the most aesthetic examples of atypical magnetic structures.<sup>[10]</sup> SMTs have attracted the attention of the scientific community, since they offer ways to design multiferroic materials at the nanoscale.<sup>[10]</sup> This class of compounds is characterized by a "vortex-like" spatial distribution (e.g. a torus disposition) of the single ion easy-axes that leads to a zero total magnetic momentum, but a non-vanishing toroidal magnetic moment. Several examples of Dy<sup>III</sup>-based polynuclear complexes (Dy<sub>3</sub> triangles,<sup>[10,11,14,15]</sup> Dy<sub>4</sub> coplanar,<sup>[16,17]</sup> coupled Dy<sub>3</sub> triangles,<sup>[18-20]</sup> Dy<sub>6</sub> wheel<sup>[21]</sup> or 3d-4f metallocycles<sup>[22]</sup>) have been reported so far with a non-magnetic Kramers doublet ground state resulting from such magnetic vortex on wheel-shaped topologies. Molecular symmetry, magnetic anisotropy direction and magnetic interactions are the key ingredients to produce SMTs.<sup>[10]</sup> In such a framework, Dy<sup>III</sup> ions are ideal candidates since it easily leads to an easy magnetic anisotropy axis.

Even if the clusters that have shown toroidal-like spin structures so far are arranged in a planar configuration, in

principle, toroidal-like spin structures, and so SMTs, might emerge as well from non-planar arrangements of the paramagnetic centers. Indeed, the requirement for a toroidal ground state is only a spatial distribution of weakly coupled magnetic moments that results in a quenching of the total momentum of the ground state, but also to a residual toroidal moment. In this regard, we investigated a novel Dy<sub>4</sub> cubane complex that shows a non-trivial toroidal magnetic moment despite its tetrahedral core. In this work, we report the structure, the magnetic characterizations along with the *ab initio* calculations and the spin Hamiltonian model which support the existence of uncommon toroidal magnetic moment in a non-planar complex (3D-SMT).

The structure of [Dy<sub>4</sub>(Bppd)<sub>4</sub>(μ<sub>3</sub>-OH)<sub>4</sub>(Pa)<sub>4</sub>(H<sub>2</sub>O)<sub>4</sub>]·0.333H<sub>2</sub>O (where BppdH=1,3-Bis(pyridin-4-yl)propane-1,3-dione and PaH=2-Picolinic acid), hereafter abbreviated **Dy<sub>4</sub>**, is represented on Figure 1. The synthesis and the details of the crystal structure are given in SI and Table S1. **Dy<sub>4</sub>** crystallizes in the centrosymmetric P4<sub>2</sub>/n tetragonal space group. The asymmetric unit is composed by one Dy<sup>III</sup> metal center, one Bppd<sup>-</sup> and one Pa<sup>-</sup> both disordered on two positions (refined to 50:50), one μ<sub>3</sub>-OH<sup>-</sup> bridge, and one terminal coordinated water molecule (Figure S1). One disordered non-coordinated water molecule completes the unit-cell. The structure of the complex is constructed as a tetranuclear architecture where one half of the vertexes of the cubane core are occupied by Dy<sup>III</sup> centers and the other half by μ<sub>3</sub>-OH<sup>-</sup> molecules (Figure 1). Each Dy<sup>III</sup> is surrounded by eight oxygen atoms (SHAPE analysis<sup>[23]</sup>: square antiprism; Table S2), two from one Bppd<sup>-</sup> ligand, two from two Pa<sup>-</sup> ligands, three from three μ<sub>3</sub>-OH<sup>-</sup> and one from a coordinated water molecule. Pa<sup>-</sup> ligands connect two lanthanide ions in a μ<sub>1,2</sub> mode on four of the six {Dy<sub>4</sub>O<sub>4</sub>} faces. Ln-O(H<sub>2</sub>O) bond lengths are greater (2.457 Å vs. 2.369 Å) than the other Ln-O bond lengths (Table S3). All the Dy-O(μ<sub>3</sub>-OH)-Dy bond angles are very similar ranging from 106.8° to 107.1°. Likewise, Dy...Dy distances within the cubane architecture are almost the same ranging from 3.83 to 3.85 Å, in line with the deviation from the ideal point group symmetry. The crystal packing is insured by π-π interactions involving aromatic rings of Bppd ligands forming a dense 3D network (Figure S2). The shortest Dy...Dy distance between two different **Dy<sub>4</sub>** (center to center) is equal to 14.0 Å ensuring no magnetic interaction between neighbors.

Room temperature χ<sub>M</sub>T value, with T the temperature in Kelvin and χ<sub>M</sub> the molar magnetic susceptibility, is just slightly smaller than expected for the <sup>6</sup>H<sub>15/2</sub> multiplet ground state with g=4/3 (52.1 vs. 56.6 cm<sup>3</sup> K mol<sup>-1</sup>) and collapses down to 2.5 cm<sup>3</sup> K mol<sup>-1</sup> on cooling down to 500 mK (Figure S3). Meanwhile, χ<sub>M</sub> passes through a rounded maximum at 2 K which clearly indicates that the ground state is non-magnetic (Figure 2). At the lowest investigated temperature, a weak increase of χ<sub>M</sub> is observed which is attributed to a low temperature paramagnetic Curie tail, due to the impurities present in the crystal. The non-magnetic ground state is confirmed by S-shaped first magnetization curve at 500 mK (Figure 2) which saturates at 19.2 Nβ (Figure S3). This value is very close to what is expected for four effective spins S<sub>eff</sub>=1/2 with g<sub>x</sub>=g<sub>y</sub>=0 and g<sub>z</sub>=20. This pattern corresponds to the stabilization of the two M<sub>J</sub>=±15/2 states. All these characteristics indicate that significant interactions operate in the cubane leading to a non-magnetic ground state with magnetic excited states with different contribution within few wavenumbers.

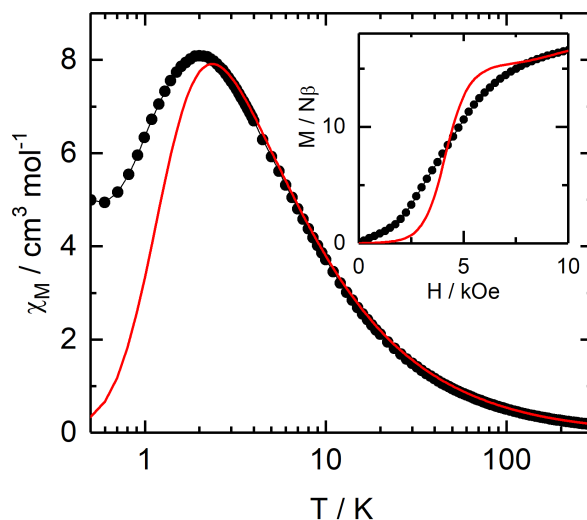


**Figure 2.** Thermal variation of the magnetic susceptibility in black dots with the calculated one (red line) according to the model developed in main text; (inset) Field variation of the magnetization at 500 mK and the calculated curve (red line).

*Ab initio* SA-CASSF/SI-SO calculations (see details in SI) have been performed to i) determine the mutual orientation of the principal magnetic axes of the Dy<sup>III</sup> ions related to their arrangement in the cubane core and ii) elucidate the magnetic interactions which stabilize the non-magnetic ground state. The magnetic properties of each Dy<sup>III</sup> ion were calculated by a diamagnetic substitution approach, *i.e.* substituting in turn the other three Dy<sup>III</sup> ions with Y<sup>III</sup> ions. The Kramers ground doublet is characterized by an axial g-tensor with a g<sub>zz</sub> ~ 19.6 in the effective spin 1/2 model (Table S4) with the first excited state at ~100 cm<sup>-1</sup> (Table S5). |±15/2> M<sub>J</sub> component (> 96%) prevails in the ground state of each Dy<sup>III</sup> ion (Table S6). The easy magnetic axes are symmetry related due to the almost perfect tetrahedral structure (Table S7). They make an angle of 30.5° with c axis (Figure S4). From the c axis perspective, it is possible to evidence the circular pattern described by the easy axes. The presence of magnetic dipole-dipole interactions (*J*<sub>dip</sub>, see SI) and exchange coupling, *J*<sub>ex</sub>, have been considered to account for the magnetic inter-ions interactions. The latter was included in the framework of the Lines model.<sup>[24]</sup> Furthermore, it was impossible to properly reproduce the experiment with enough accuracy either with *J*<sub>ex</sub>=0 (*i.e.* only dipolar interactions) or with a unique *J*<sub>ex</sub> (Figure S5). To clarify the magnetic exchange coupling scheme, the following spin Hamiltonian was used (the subscript « ex » is omitted):

$$H_{spin} = -J_1(\hat{S}_1 \cdot \hat{S}_2 + \hat{S}_2 \cdot \hat{S}_3 + \hat{S}_3 \cdot \hat{S}_4 + \hat{S}_4 \cdot \hat{S}_1) - J_2(\hat{S}_1 \cdot \hat{S}_3 + \hat{S}_2 \cdot \hat{S}_4)$$

with *J*<sub>1</sub> and *J*<sub>2</sub> referring to the exchange couplings when μ<sub>3</sub>-OH and carboxylate or only μ<sub>3</sub>-OH bridging groups are involved, respectively, S<sub>i</sub>'s are the effective spin operators at Dy<sup>III</sup> sites (Figure 3). The dipolar interaction is calculated routinely in the point-dipole approximation. All the calculations were performed with the POLY\_ANISO routine<sup>[25,26]</sup> and homemade fitting code, with the inclusion of the g tensors for each Dy center calculated separately (Table S4). With this model both the crystallographic

disorder on each metal site and the non-collinearity of the single-ion  $g$  tensors are considered. In this framework, the resulting low-lying 16 states are arranged in four groups of degenerate states (Figure 3). For the sake of simplicity, the spatial disposition of the single magnetic moments (left-hand side in Figure 3) for each group of states can be labeled using the collinear “up” ( $\uparrow$ ) and “down” ( $\downarrow$ ) notation. Remarkably, the total magnetic moment of the ground state  $|\uparrow\downarrow\downarrow\rangle$  is close to 0 (effective  $g=0.46$ ), while excited states have a non-zero total magnetic moment. Looking at the spins configuration of the ground state along the  $c$  axis (Figure 3), the toroidal arrangement of the magnetic moments emerges.

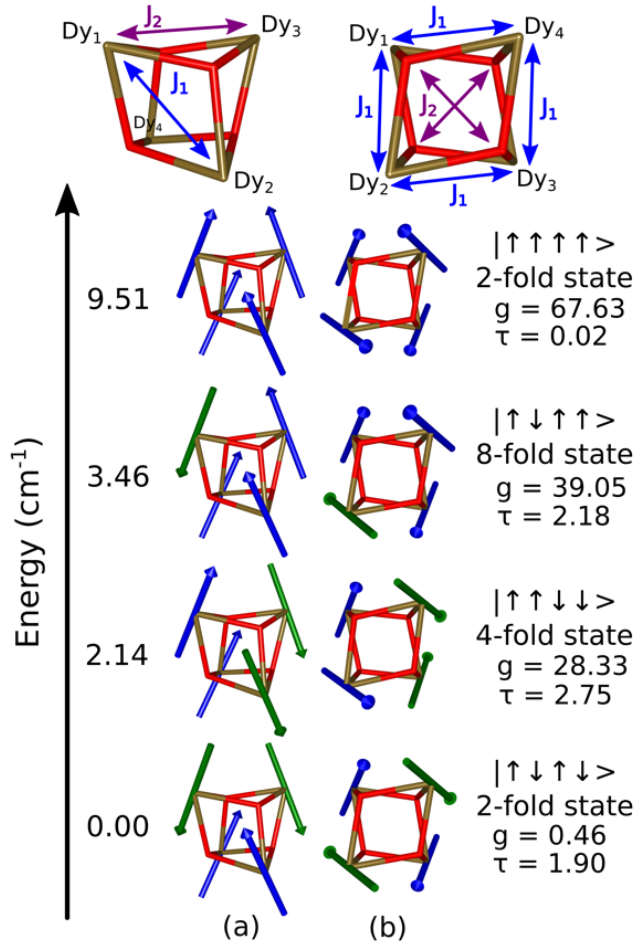


**Figure 3.** Coupling scheme within  $\text{Dy}_4$  (top) with the calculated energy state degeneracies (bottom) along two directions (x axis view for (a); c axis view for (b)) with  $g_{zz}$ -values in the effective spin 1/2 framework and calculated toroidal moment  $\tau$  (in  $\beta\cdot\text{\AA}$ ).

To determine under which condition state  $|\uparrow\downarrow\uparrow\downarrow\rangle$  becomes the ground state, we mapped the energies of the low-lying states for  $J_1$  and  $J_2$  ranging from  $-0.5$  to  $+0.5$   $\text{cm}^{-1}$ . The resulting surfaces, called Exchange Energy Surfaces (EES) in analogy with the widely used Potential Energy Surfaces (PES), are plotted on Figure 4. The ground state is always non-magnetic for  $J_1 < 0$  and  $J_2 > 0$ . For  $J_1 < 0$  and  $J_2 < 0$  (only antiferromagnetic couplings) there is a competition between states  $|\uparrow\downarrow\uparrow\downarrow\rangle$  and  $|\uparrow\uparrow\downarrow\downarrow\rangle$ . In this subset of values, states  $|\uparrow\downarrow\uparrow\downarrow\rangle$  or  $|\uparrow\uparrow\downarrow\downarrow\rangle$  are stabilized when  $J_1$  or  $J_2$  dominates, respectively. However, on

the basis of the well-known efficiency of the super-exchange pathway given by the carboxylate ligands,  $J_1$  is therefore expected to be dominating in  $\text{Dy}_4$ .<sup>[27]</sup> Such results point out the necessity to verify the presence of equivalent set of exchange parameters able to reproduce in the most accurate way as possible the experiment. Even if only seldom performed,<sup>[28]</sup> such a detailed analysis of the EES's is mandatory whenever in presence of potentially high correlated set of parameters (Figure 4). We finally identified a set of  $J$  values ( $J_1 = -0.27$   $\text{cm}^{-1}$  and  $J_2 = -0.09$   $\text{cm}^{-1}$ ) that match reasonably well the maximum on the  $\chi_M$  vs. T curve as well as the inflexion point on the M vs. H curve (Figures 2 and S5). The slight deviation at low T may be ascribed to small amount of paramagnetic impurities and structural disorder on the ligands that are not taken into account in the calculations. The selected set of exchange parameters is not, of course, the unique set which can reproduce the experimental data, but surely it is the most sound on the basis of the ab initio results. Indeed, when one of the most important parameters is fixed (the energy gap between the ground and first excited states), all other used sets of parameters fail to reproduce the experiment (Figure S5). The energy diagram and the calculated total  $g$ -values in the effective spin 1/2 framework are provided on Figure 3: The ground state is non-magnetic, even if its global  $g$ -value is not strictly zero due to the disorder in the crystal structure that lower the symmetry. To confirm this, we ran a calculation on a symmetrized spin Hamiltonian ( $T_d$  symmetry) resulting in a strict diamagnetic ground state (see SI, Table S8). Back to the main model, the first excited states  $|\uparrow\uparrow\downarrow\downarrow\rangle$  ( $g=28.33$ ) lie 2.14  $\text{cm}^{-1}$  above the ground state, while the third and fourth excited states are at 3.46  $\text{cm}^{-1}$  ( $g=39.05$ ) and 9.51  $\text{cm}^{-1}$  ( $g=67.63$ ), respectively. One must notice that for all excited states, global  $g$  tensors are not collinear (Figure S6). In order to confirm that state  $|\uparrow\downarrow\uparrow\downarrow\rangle$  is not only non-magnetic but possesses a non-zero toroidal moment, we calculated the total spin  $\vec{S}_{\text{tot}} = \sum_i \vec{S}_i$  and the toroidal moment  $\vec{\tau} \propto \sum_i \vec{r}_i \times \vec{S}_i$ , respect to the center of mass of the metal core (as a reference the same quantities were calculated for the archetypal  $\text{Dy}_3$  triangle,<sup>[15]</sup> see Table S9). State  $|\uparrow\downarrow\uparrow\downarrow\rangle$  presents a quenching of the total spin but a non-zero  $\tau$  (net toroidal moment), while state  $|\uparrow\uparrow\downarrow\downarrow\rangle$  has both non-zero  $\tau$  and  $S_{\text{tot}}$  (mixed-moment SMT).

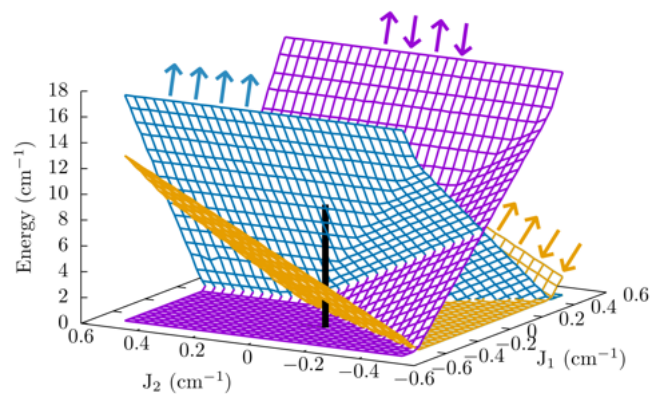


**Figure 4.** EES for states  $|\uparrow\downarrow\uparrow\downarrow\rangle$ ,  $|\uparrow\uparrow\downarrow\downarrow\rangle$  and  $|\uparrow\uparrow\uparrow\uparrow\rangle$ . State  $|\uparrow\downarrow\uparrow\downarrow\rangle$  has been omitted for clarity. The vertical black segment corresponds to the best agreement with the experiment ( $J_1 = -0.27$   $\text{cm}^{-1}$  and  $J_2 = -0.09$   $\text{cm}^{-1}$ ).

$\text{Dy}_4$  shows frequency dependent ac susceptibility in the 2-11 K temperature in the absence of an external dc field (Figure S7), the signature of the slowing down of the magnetic moment. According to the calculated energy diagram of  $\text{Dy}_4$  (*vide supra*),

even at 2 K not only the non-magnetic ground-state is populated but the other states are also involved. As a result, the relaxation of the magnetic moment implies several states with different processes. Nevertheless, the experimental data can be analyzed in the frame of the extended Debye model which feature one main relaxation with a relatively narrow distribution ( $\alpha < 0.3$ ) (see SI, Figure S8, Table S10). While a thermally dependent process dominates at high temperature, the relaxation time tends to become thermally independent below 4 K. The energy diagram which results from the coupling between local magnetic moments impacts, in a complex manner, the in-field relaxation dynamics. At 2 K, the in-field behavior of  $\chi_M'$  in the 1-1000 Hz frequency window is plotted on Figure 6. It reflects the in-field evolution of the relaxation time which is not monotonic. The slowing down at low field is commonly observed in mononuclear SMMs. At higher field than 1 kOe the relaxation time decreases as the surface plot moves to higher frequencies (Figure S9). The black line at high frequencies (1000 Hz) shows two maxima at 2.8 and 4 kOe. These fields correspond to the crossings between the first three states ( $|\uparrow\uparrow\downarrow\rangle$ ,  $|\uparrow\uparrow\downarrow\rangle$  and  $|\uparrow\downarrow\uparrow\rangle$ ) in agreement with Zeeman energy diagrams calculated with the magnetic applied along the principal axis of state  $|\uparrow\uparrow\uparrow\rangle$  (4.3 kOe, Figure S10) and along one of the principal axes of state  $|\uparrow\uparrow\downarrow\rangle$  (3.2 kOe, Figure S11). This allows multiple relaxation pathways to the global magnetic moment.

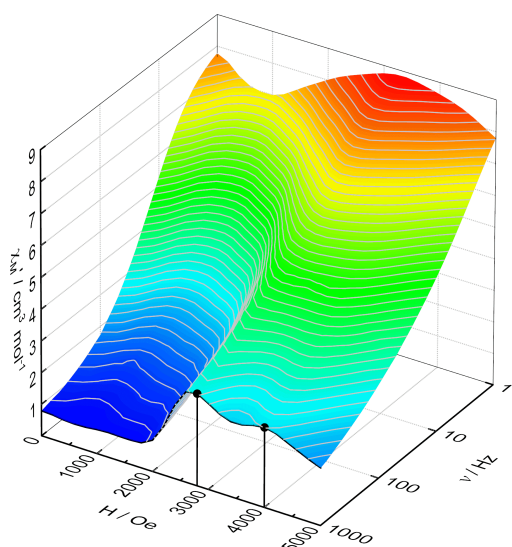


**Figure 6.** Variation of the in-phase component ( $\chi_M'$ ) at 2 K with the frequency of the oscillating field ( $\nu$ ) and the external dc field ( $H$ ). The thick black line corresponds to  $\chi_M'$  values at 1000 Hz and the two dots to the observed maxima at 2.8 and 4 kOe.

Significant toroidal magnetic moment in a  $Dy_4$  cubane complex associated to a non-magnetic ground state has been characterized in detail by magnetometry and state-of-art *ab initio* computational methods. A deep analysis of the low-lying energy states resulting from the specific coupling scheme allows to reliably identify the best set of parameters to properly reproduce the magnetic data. The computed energy ladder also suggests that in such a class of systems, the magnetic nature of the ground state could be easily modulated by altering the  $J_1/J_2$  ratio and, therefore, by slight changes in the ligand nature or by external perturbations (*i.e.* pressure). As far as we know, this is one of the first cases in which a non-magnetic toroidal ground state is found in a 3D topology (3D-SMT). This strongly differs

from ferrotoroidic systems composed by two connected frustrated rings (interacting 2D-SMT).<sup>[29]</sup> These findings pave the way to the design of original three-dimensional toroids as new objects in molecular spintronic.

## Acknowledgements

D. G. is grateful for the PhD fellowship from University Claude Bernard Lyon 1. Additional support was provided by the Région Rhône-Alpes (CMIRA2015). G. F. G. gratefully acknowledges the European Commission through the ERC-AdG MolNano-Mas (project no. 267746) and the ANR (ANR-13-BS07-0022-01) for financial support. V. M. is thankful to ERC (project no. 725184) for fundings. B. L. G. thanks the French GENCI/IDRIS-CINES center for high-performance computing resources. COST Action Molspin (CA 15128) is also acknowledged.

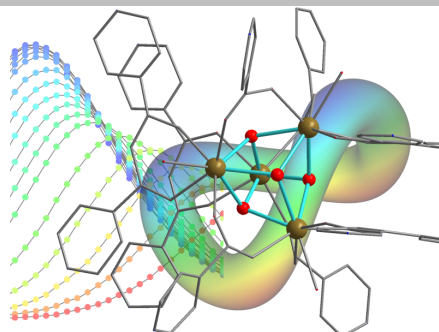
**Keywords:** single molecule toroids • lanthanide • dysprosium • cubane • ab initio calculations

- [1] a) R. Sessoli, D. Gatteschi, A. Caneschi, M. A. Novak, *Nature* **1993**, *365*, 141-143; b) R. Sessoli, H. L. Tsai, A. R. Schake, S. Wang, J. B. Vincent, K. Folting, D. Gatteschi, G. Christou, D. N. Hendrickson, *J. Am. Chem. Soc.* **1993**, *115*, 1804-1816.
- [2] N. Ishikawa, M. Sugita, T. Ishikawa, S. Koshihara, Y. Kaizu, *J. Am. Chem. Soc.* **2003**, *125*, 8694-8695.
- [3] D. N. Woodruff, R. E. P. Winpenny, R. A. Layfield, *Chem. Rev.* **2013**, *113*, 5110-5148.
- [4] A. Cornia, O. Seneor, *Nature Materials* **2017**, *16*, 505-506.
- [5] S. Sanvito, *Nature Physics* **2010**, *6*, 562-564.
- [6] J. Tang, P. Zhang, *Lanthanide Single-Molecule Magnets* Springer-Verlag: Heidelberg, 2015.
- [7] S. T. Liddle, J. van Slageren, *Chem. Soc. Rev.* **2015**, *44*, 6655-6669.
- [8] F. Pointillart, K. Bernot, S. Golhen, B. Le Guennic, T. Guizouarn, L. Ouahab, O. Cador, *Angew. Chem. Int. Ed.* **2015**, *54*, 1504-1507.
- [9] Y.-C. Chen, J.-L. Liu, W. Wernsdorfer, D. Liu, L. Chibotaru, X.-M. Chen, M.-L. Tong, *Angew. Chem. Int. Ed.* **2017**, *56*, 4996-5000.
- [10] L. Ungur, S.-Y. Lin, J. Tang, L.F. Chibotaru, *Chem. Soc. Rev.* **2014**, *43*, 6894-6905.
- [11] J. Tang, P. Zhang, *Polynuclear Lanthanide Single Molecule Magnets*. In *Lanthanides and Actinides in Molecular Magnetism*; Layfield, R. A., Murugesu, M., Eds.; VCH: Weinheim, 2015, pp 61-88.
- [12] J. D. Rinehart, M. Fang, W. J. Evans, J. R. Long, *Nature Chem.* **2011**, *3*, 538-542.
- [13] Y.-N. Guo, G.-F. Xu, W. Wernsdorfer, L. Ungur, Y. Guo, J. Tang, H.-J. Zhang, L. F. Chibotaru, A. K. Powell, *J. Am. Chem. Soc.* **2011**, *133*, 11948-11951.
- [14] J. Tang, I. Hewitt, N. T. Madhu, G. Chastanet, W. Wernsdorfer, C. E. Anson, C. Benelli, R. Sessoli, A. K. Powell, *Angew. Chem., Int. Ed.* **2006**, *45*, 1729-1733.
- [15] J. Luzon, K. Bernot, I. J. Hewitt, C. E. Anson, A. K. Powell, R. Sessoli, *Phys. Rev. Lett.*, **2008**, *100*, 247205.
- [16] P.-H. Guo, J.-L. Liu, Z.-M. Zhang, L. Ungur, L. Chibotaru, J.-D. Leng, F.-S. Guo, M.-L. Tong, *Inorg. Chem.* **2012**, *51*, 1233-1235.
- [17] A. Gusev, R. Herchel, I. Nemeč, V. Shul'gin, I. L. Eremanko, K. Lyssenko, W. Linert, Z. Trávníček, *Inorg. Chem.* **2016**, *55*, 12470-12476.
- [18] I. J. Hewitt, J. Tang, N. T. Madhu, C. E. Anson, Y. Lan, J. Luzon, M. Etienne, R. Sessoli, A. K. Powell, *Angew. Chem. Int. Ed.* **2010**, *49*, 6352-6356.
- [19] X.-L. Li, J. Wu, J. Tang, B. Le Guennic, W. Shi, P. Cheng, *Chem. Commun.*, **2016**, *52*, 9570-9573

- [20] S.-Y. Lin, W. Wernsdorfer, L. Ungur, A. K. Powell, Y.-N. Guo, J. Tang, L. Zhao, L.F. Chibotaru, H.-J. Zhang, *Angew. Chem. Int. Ed.* **2012**, *51*, 12767-12771.
- [21] L. Ungur, S. K. Langley, T. N. Hooper, B. Moubaraki, E. K. Brechin, K. S. Murray, L. F. Chibotaru, *J. Am. Chem. Soc.* **2012**, *134*, 18554–18555.
- [22] J. Wu, X.-L. Li, M. Guo, L. Zhao, Y.-Q. Zhang, J. Tang, *Chem. Commun.* **2018**, *54*, 1065-1068.
- [23] M. Llunell, D. Casanova, J. Cirera, J. M. Bofill,; P. Alemany, S. Alvarez, SHAPE (Version 2.1) **2013**.
- [24] M. E. Lines, *J. Chem. Phys.* **1971**, *55*, 2977.
- [25] L. F. Chibotaru, L. Ungur, A. Soncini, *Angew. Chem. Int. Ed.* **2008**, *47*, 4126-4129.
- [26] L. Ungur, W. Van den Heuvel, L. F. Chibotaru, *New J. Chem.* **2009**, *33*, 1224–1230.
- [27] J. H. Rodriguez, J. K. McCusker, *J. Chem. Phys.* **2002**, *116*, 6253-6270.
- [28] D. Krishnamurthy, A. Sarjeant, D. P. Goldberg, A. Caneschi, F. Totti, L. N. Zakharov, A. L. Rheingold, *Chem. Eur. J.* **2005**, *11*, 7328-7341.
- [29] K. R. Vignesh, A. Soncini, S. K. Langley, W. Wernsdorfer, K. S. Murray, G. Rajaraman, *Nature Commun.* **2017**, *8*, 1023.

## COMMUNICATION

**3D magnetic toroics:** Molecular materials that possess a toroidal moment associated to a non-magnetic ground state are known as Single-Molecule Toroics (SMTs) and are usually planar molecules. It is herein observed in a Dy<sub>4</sub> cubane, transposing this property to a tridimensional structure (3D-SMT).



*Guglielmo Fernandez Garcia, Djamilla Guettas, Vincent Montigaud, Paolo Larini, Roberta Sessoli, Federico Totti, Olivier Cador,\* Guillaume Pilet,\* and Boris Le Guennic\**

**A Dy<sub>4</sub> Cubane: A New Member in the Single-Molecule Toroics Family**